

An overview of some characteristic numerical models for concrete

Mirela Galić and Pavao Marović

University of Split, Faculty of Civil Engineering, Architecture and Geodesy,
Matice hrvatske 15, HR-21000 Split, CROATIA
e-mail: mirela.galic@gradst.hr; marovic@gradst.hr

SUMMARY

On the basis of experimental testing of behaviour of concrete, reinforced concrete and prestressed concrete structures, various phenomena were observed; in the first place, highly non-linear and inelastic behaviour of concrete. Since it is hard to include all the phenomena and changes that occur in concrete, a large number of numerical models for concrete were developed to describe different states of the problem under consideration, with the tendency to include in these analyses the changes that are dominant in the observed problem. This paper will give a brief overview of some characteristic numerical models for concrete, developed so far, with a short overview of their advantages and disadvantages, i.e. possibilities and limitations. The models were classified depending on the formulation of the constitutive laws. Models were chosen to demonstrate the diversity of modelling and specifics of their application.

Key words: concrete, constitutive concrete model, numerical concrete model, plasticity.

1. INTRODUCTION

On the basis of experimental testing of behaviour of concrete, reinforced concrete and prestressed concrete structures, various phenomena were observed; namely: non-linear and non-elastic behaviour of concrete and reinforcement; concrete damages that cause degradation of the linear-elastic constants in the material matrix; non-linear behaviour of concrete and reinforcement when limit stress is exceeded; multi-axial and non-uniform strain distribution which induces the development of cracks in concrete; concrete and reinforcement interaction; hardening of non-cracked concrete between the two adjacent cracks due to tensile stresses; different yield point when a reinforcement incorporated in concrete is analyzed compared to the one when reinforcement is analyzed separately. When

developing computer programmes for the analyses and computation of reinforced concrete and prestressed concrete structures, a mathematical model shall be devised, which will include as many of these impacts, and implemented in a computer programme to get the most faithful response of the structure to the applied load. Since it is hard to incorporate all the changes that occur in concrete, a large number of numerical models for concrete have been developed to describe various situations, with the tendency to include in these analyses the changes that are dominant in the observed problem [1-3].

In this sense, this paper gives a brief overview of the some characteristic numerical models for concrete, with a short overview of their advantages and disadvantages, i.e. possibilities and limitations.

2. CLASSIFICATION OF THE NUMERICAL MODELS FOR CONCRETE

Depending on the observation level, concrete shows different physical and geometrical properties. The observed size scales for concrete can be typically subdivided into hierarchical levels: atomic level, micro-level, meso-level and macro-level (see Fig. 1 according to Ref. [4]). So, the main task is to create such numerical model which will describe concrete adequately on the observed or prescribed level.

Considering material modelling on the micro- and macro-level the numerical models of concrete can be divided into two large groups:

1. Models of concrete which are mathematically formulated by using stress and strain invariants creating constitutive laws connecting strain tensor and stress tensor on the macro-level. Depending on the type of these relations, they can be divided into few large groups incorporating more precise divisions. These are:
 - * models based on the theory of elasticity,
 - * models based on the theory of elasto-plasticity and/or theory of plasticity, which can be single-surface or multi-surface,
 - * endocrone models,
 - * damage models,
 - * models based on the theory of fracture mechanics.
2. Models of concrete where the relationship between components of the stresses and components of the strains is created on the micro-level afterwards connected on the macro-level into stress tensor by using principle of virtual work.

2.1 Surface plasticity models

The need for more realistic description of the concrete initiate the development of large number of models which gives the broad spectrum of answers in describing the behaviour of this heterogeneous material under different loading conditions. These

behaviours under different stress states are suitable to follow in characteristic plane or planes. This is the reason why this group of models get name surface models. Some of them will be shown in this paper.

2.1.1 Single-surface plasticity models

Etse and Willam [5, 6] develop an isotropic plasticity model which can be considered to be the basic single-surface plasticity model of concrete. The loading surfaces are described as:

$$f_{EW} = (p, r, \theta, k, c) = \left\{ (1-k) \left[\frac{p}{f_{cu}} + \frac{rg(\theta)}{\sqrt{6}f_{cu}} \right]^2 + \sqrt{\frac{3}{2}} \frac{rg(\theta)^2}{f_{cu}} \right\} + \frac{k^2 m}{f_{cu}} \left[p + \frac{rg(\theta)}{\sqrt{6}} \right] - k^2 c = 0 \quad (1)$$

where p , r and θ are invariants of the stress tensor, and f_{cu} is the uniaxial compressive strength of the concrete. Function $g(\theta)$ defines the deviatoric shape of the yield surface. The parameter k , i.e. the normalized strength variable, controls the pre-peak behaviour of the concrete while the cohesion parameter c controls the post-peak behaviour of the concrete. The parameter m is called frictional parameter and defines the shape of the yield surface in the meridian plane of the softening regime. Variables which define hardening and softening are introduced in dependence on ultimate stress. The evolution of the loading surfaces in the pre-peak regime is shown in Figure 2.

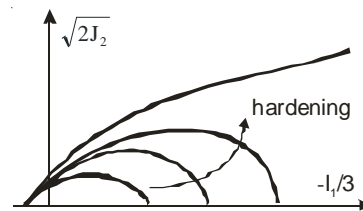


Fig. 2 Etse-Willam model

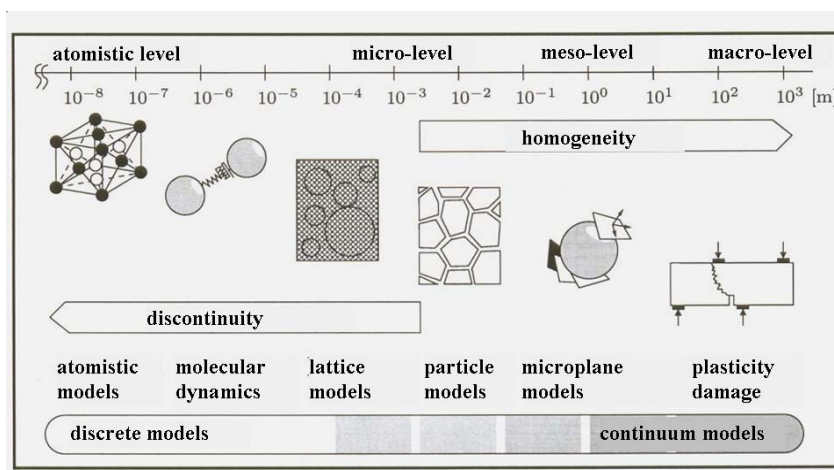


Fig. 1 Scale levels for concrete constitutive modelling [4]

Extended Leon Model (ELM) [5, 6] is de facto extended Etse-William model. It belongs to the group of single-surface plasticity models. The loading surfaces are described as:

$$\begin{aligned}
 f_{EW} = (p, r, \theta, q_h, q_s) = & \\
 = & \left\{ \left(1 - \frac{\bar{q}_h}{f_{cu}} \right) \left[\frac{p}{f_{cu}} + \frac{rg(\theta, e)}{\sqrt{6}f_{cu}} \right]^2 + \sqrt{\frac{3}{2}} \frac{rg(\theta, e)^2}{f_{cu}} \right\}^2 + \\
 & + \left(\frac{\bar{q}_h}{f_{cu}} \right)^2 m(q_s) \left[\frac{p}{f_{cu}} + \frac{rg(\theta, e)}{\sqrt{6}f_{cu}} \right] - \left(\frac{\bar{q}_h}{f_{cu}} \right)^2 \frac{\bar{q}_s}{f_{tu}} = 0
 \end{aligned} \tag{2}$$

having in mind that $\bar{q}_h = f_{cy} - q_h$ and $\bar{q}_s = f_{tu} - q_s$ where: p is the hydrostatic pressure, r is the radius of the deviatoric plane, θ is the Lode angle, f_{cy} is the elastic limit of concrete under compression loading, while f_{cu} and f_{tu} are uniaxial compressive and uniaxial tensile strength of the concrete.

Figure 3 shows loading surfaces in the principal stress space for different loading states and in the pre-peak and post-peak regimes in the deviatoric planes. The deviatoric shape of the loading surface is described by the elliptic function $g(\theta, e)$ [7] where e is the parameter of eccentricity describing transformation of the loading surface from circular ($e=1.0$) to almost triangular ($e=0.5$) shape.

Extended Leon model incorporates parameters q_h and q_s (Figure 3) which controls hardening and softening behaviour of the concrete. Adequate functions include two internal variables α_h and α_s by which material behaviour is traced.

2.1.2 Multi-surface plasticity models

In the multi-surface plasticity models [8] at least two loading surfaces are defined, i.e. one for the

description of the failure criterion when concrete is exposed to the compression stresses and one for the description of the crack development.

One of the most popular multi-surface plasticity models, because of its simple formulation, is a combination of the Drucker-Prager and Rankine models. It consists of a Drucker-Prager (DP) yield surface for the description of concrete subjected to compressive loading and Rankine (RK) surfaces for the description of the tensile behaviour of concrete. As Drucker-Prager criterion is calibrated by means of uniaxial and a biaxial compression tests a great number of modifications are proposed accounting for the influence of confinement on the hardening/softening behaviour, i.e. for describing the behaviour of the concrete in different compression-tension regions. In the Westergard space a maximum tensile stress criterion (Rankine criterion), within the framework of the smeared cracks, is used to determine the tensile strength of concrete for triaxial states of cracks:

$$\begin{aligned}
 f_{RK,A}(\sigma_A, q_{RK}) = \sigma_A - \bar{q}_{RK} \\
 \text{with: } \bar{q}_{RK} = f_{tu} - q_{RK}
 \end{aligned} \tag{3}$$

Index $A = 1, 2, 3$ denotes axis of principal stresses, \bar{q}_{RK} is uniaxial tensile stress, and q_{RK} is an isotropic stress-like internal variable. Ductility of the concrete exposed to the triaxial compression is described by the Drucker-Prager function expressed in the invariant formulation as:

$$\begin{aligned}
 f_{DP}(\sigma, q_{DP}) = \sqrt{J_2} - k_{DP} I_1 - \frac{\bar{q}_{DP}}{\beta_{DP}} \\
 \text{with: } \bar{q}_{DP} = f_{cy} - q_{DP}
 \end{aligned} \tag{4}$$

where f_{cy} represents the elastic limit of concrete, while parameters k_{DP} and β_{DP} are obtained from the peak strengths of uniaxial (f_{cu}) and biaxial (f_{cb}) loading. For relation $f_{cb} / f_{cu} = 1.16$, the parameters k_{DP} and β_{DP} have values $k_{DP} = -0.07$ and $\beta_{DP} = 1.97$ [9].

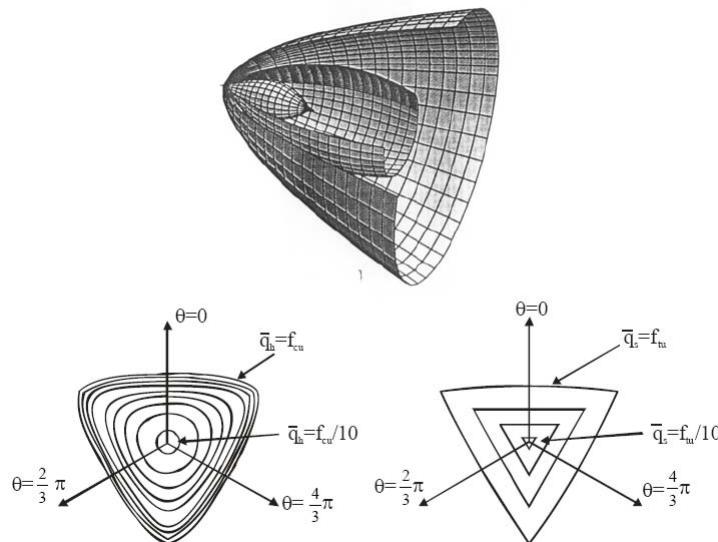


Fig. 3 Extended Leon model (according to Ref. [2])

The strain-like internal variables α_{DP} and α_{RK} have been introduced to describe micro-structural changes of concrete, i.e. hardening and softening of concrete, as:

$$\alpha_{DP} = \gamma_{DP} \frac{\partial f_{DP}}{\partial q_{DP}}, \quad \alpha_{RK} = \gamma_{RK,A} \frac{\partial f_{RK,A}}{\partial q_{RK}} \quad (5)$$

The flow rule for the evolution of the plastic strain tensor ε^p is given by:

$$\varepsilon^p = \gamma_{DP} \frac{\partial f_{DP}}{\partial \sigma} + \sum_{A=1}^3 \gamma_{RK,A} \frac{f_{RK,A}}{\sigma_A} \quad (6)$$

Decrease of the tensile strength, i.e. softening behaviour of concrete, is accounted for by an exponential law, as:

$$q_{RK} = f_{tu} e^{\alpha_{rk} / \alpha_{rk,u}} \quad (7)$$

A model similar to the previous one is a combination of the Drucker-Prager model and “Tension Cut-of” criterion. It consists of a Drucker-Prager (DP) yield surface for the description of concrete subjected to compressive loading and “Tension Cut-of” criterion (TC) for the description of the tensile behaviour of concrete. As “Tension Cut-of” criterion can be considered as a restriction of the Rankine criterion the same mathematical description can be used with the substitutions in the tensile stress criterion as:

$$f_{TC}(\sigma, q_{TC}) = \sigma_A - q_{TC}, \quad (8)$$

$$\text{where: } q_{TC} = \frac{f_{tu}}{3} - q_{RK}$$

The parameter α is now defined according to $\alpha_{TC} = \gamma_{TC} \frac{\partial f_{TC}}{\partial q_{TC}}$, while the flow rule for the evolution of the plastic strain tensor ε^p is now given as:

$$\varepsilon^p = \gamma_{DP} \frac{\partial f_{DP}}{\partial \sigma} + \sum_{A=1}^3 \gamma_{TC} \frac{f_{TC}}{\sigma} \quad (9)$$

As can be concluded from the beforementioned discussions, for describing the behaviour of concrete in different stress states, i.e. in different planes, these models requires the knowledge of some material and model parameters which are obtained by experimental testing. These parameters are shown in Table 1.

Model Galić-Marović or Modified Mohr-Coulomb – Rankine model is multi-surface plasticity model (Figure 4) where nonlinear behaviour of concrete is described by a new elastoplastic modified material model which is based on the Mohr-Coulomb law for dominant compression stresses and the Rankine law for dominant tensile stresses [2, 10] and with two different functions for describing hardening and softening of concrete. Nonlinear triaxial behaviour of concrete is involved in this model, including all dominant influences in concrete such as yielding in compression, cracking in tension, softening and hardening of concrete.

Table 1. Basic parameters for defining behaviour of concrete with plasticity models

Material parameters	Model parameters
Modulus of elasticity, E	Elastic limit of concrete $f_{cy} = 0.4 f_{cu}$
Poisson ratio, ν	Biaxial compressive strength $f_{cb} = 1.15 f_{cu}$
Uniaxial tensile strength, f_{tu}	Fracture energy $G_f^{II} = 50 G_f^I$
Uniaxial compressive strength, f_{cu}	Strain at maximal uniaxial strength $\varepsilon_m = 0.0022$, used for $\alpha_{DP} = \varepsilon_m \cdot f_{cu} / E$
Shear modulus, G	

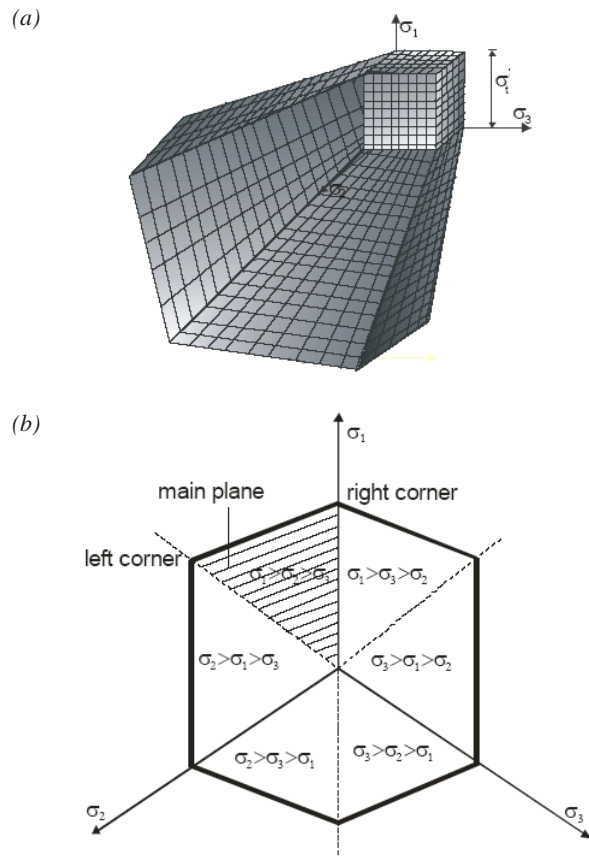


Fig. 4 Multi-surface presentation of model for concrete (a) Three-dimensional presentation, (b) Presentation in the deviatoric plane for compression influences

The behaviour of concrete under dominant tensile stresses is described by the modified Rankine material law (Figure 5). Some modifications have been performed with the cracking criterion and with the tensile strength reduction when the dominant tensile stresses appear in the combination with compressive stresses. The model includes functions for describing the tensile softening of cracked concrete. The obtained data from the performed experiments show that some part of the shear stresses is transferred across the cracks due to the influence of reinforcement bars and aggregate interlocking. So, in the presented model these influences are taken into account by the reduction of the shear modulus.

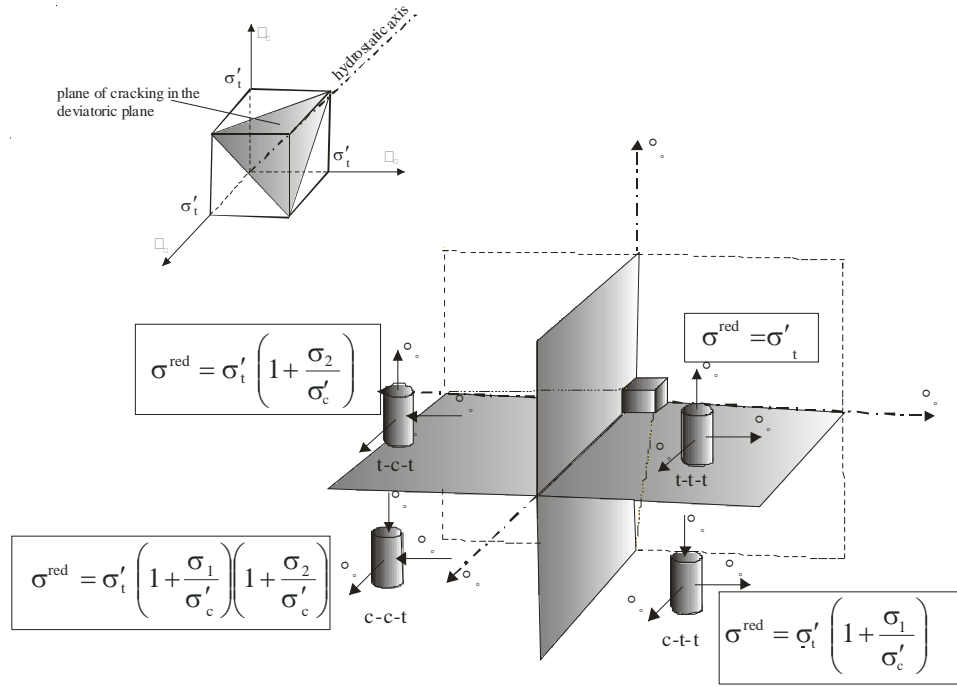


Fig. 5 Fracture model for concrete

Nonlinear behaviour of concrete for dominant compression stresses is described by an elastoplastic material model which is based on the Mohr-Coulomb law. At multi-surface model presentation the yielding surface is composed of six planes in the area of main stresses defined by the following expressions:

$$\begin{aligned}
 f_1 &= (\sigma_1 - \sigma_3) + (\sigma_1 + \sigma_3) \sin \varphi - 2c \cos \varphi & \text{for } \sigma_1 > \sigma_2 > \sigma_3 \\
 f_2 &= (\sigma_2 - \sigma_3) + (\sigma_2 + \sigma_3) \sin \varphi - 2c \cos \varphi & \text{for } \sigma_2 > \sigma_1 > \sigma_3 \\
 f_3 &= (\sigma_2 - \sigma_1) + (\sigma_2 + \sigma_1) \sin \varphi - 2c \cos \varphi & \text{for } \sigma_2 > \sigma_3 > \sigma_1 \\
 f_4 &= (\sigma_3 - \sigma_1) + (\sigma_3 + \sigma_1) \sin \varphi - 2c \cos \varphi & \text{for } \sigma_3 > \sigma_2 > \sigma_1 \\
 f_5 &= (\sigma_3 - \sigma_2) + (\sigma_3 + \sigma_2) \sin \varphi - 2c \cos \varphi & \text{for } \sigma_3 > \sigma_1 > \sigma_2 \\
 f_6 &= (\sigma_1 - \sigma_2) + (\sigma_1 + \sigma_2) \sin \varphi - 2c \cos \varphi & \text{for } \sigma_1 > \sigma_3 > \sigma_2
 \end{aligned} \tag{10}$$

Experimental studies have shown that for materials sensitive to hydrostatic pressure in the process of formation and development of plastic strains, such as concrete, the volume plastic strain is less than the one obtained by a non-associated flow rule. Hence, the plastic potential function is defined as:

$$Q = (\sigma_1 - \sigma_3) + (\sigma_1 + \sigma_3) \sin \psi - 2c \cos \psi \quad \text{for } \sigma_1 > \sigma_2 > \sigma_3 \tag{11}$$

where ψ is the dilatancy angle by which the yielding function will be improved (Figure 6a). By forming the plastic potential function, the application of the non-associated flow rule is made possible where the flow vector is defined as normal to the plastic potential surface Q_i . The calculation of the plastic strain increment for a non-associated flow rule is analogous to the calculation for the associated flow rule.

In the mentioned expressions, the angle of friction is exchanged for the dilatancy angle. As the angle φ has to be changed due to the plastic potential definition it is suitable to describe hardening using cohesion:

$$f_1 = (\sigma_1 - \sigma_3) + (\sigma_1 + \sigma_3) \sin \varphi - 2c(\bar{\varepsilon}^P) \cos \varphi \quad \text{for } \sigma_1 > \sigma_2 > \sigma_3 \tag{12}$$

In this equation, c is the function of equivalent accumulated plastic strains obtained from a uniaxial test and can be expressed as:

$$c(\bar{\varepsilon}^P) = \frac{1 - \sin \varphi}{2 \cos \varphi} \sigma(\bar{\varepsilon}^P)$$

where the relation between σ and $\bar{\varepsilon}^P$ was proposed by Meschke [11] and is given as:

$$\frac{\sigma(\bar{\varepsilon}^P)}{\sigma_c} = f_1(\bar{\varepsilon}^P) = c_y + (1 - c_y) \sqrt{1 - \left(\frac{\bar{\varepsilon}_c^P - \bar{\varepsilon}^P}{\bar{\varepsilon}_c^P} \right)^2} \tag{13}$$

where $\bar{\varepsilon}_c^P$ is the value of $\bar{\varepsilon}_c^P$ at $\sigma = \sigma_y$, and c_y is cohesion on the initial yield surface that bounds the initial elastic response, Figure 6b.

The softening law is controlled by the function for uniaxial compression which was originally proposed by Gysel and Taerwe [12] in the form:

$$\frac{\sigma(\bar{\varepsilon}^P)}{\sigma_c} = f_2(\bar{\varepsilon}^P) = \left[1 + \left(\frac{n_1 - 1}{n_2 - 1} \right)^2 \right]^{-2} \quad (14)$$

where $n_1 = \bar{\varepsilon}^P / \bar{\varepsilon}_c^P$ and $n_2 = (\bar{\varepsilon}_c^P + t) / \bar{\varepsilon}_c^P$. Parameter t controls the slope of the softening function. The complete elastic, hardening and softening functions of concrete with respect to the total plastic strains are presented in Figure 6c.

Advantages of this model are: a multi-surface presentation is implemented which permits the rapid convergence of the mathematical procedure; all influences are described by the elementary parameters for material which can be obtained by a standard uniaxial test so that the very complex behaviour of reinforced concrete structures can be described simply and effectively but with a sufficiently accurate model including all dominant influences in concrete such as yielding in compression, cracking in tension, softening and hardening of concrete.

Generally, multi-surface models are adequate for describing the reinforced concrete cross-sections i.e. reinforced concrete structures, especially in the situations when the overstep of allowable stresses, i.e. reaching the ultimate strength, and the collapse of the cross-section occur over reinforcement.

2.2 Damage models

Voyiadjis - Abu-Lebdech model [7] (Figure 7) introduces two criteria: the bounding surface F_{VA} and the loading surface f_{VA} , which are described as follows:

$$F_{VA}(\sigma, \bar{D}) = aJ_2 + \lambda\sqrt{J_2} + bI_1 - g(\bar{D}) = 0 \quad -$$

bounding surface

$$f_{VA}(\sigma, \bar{D}) = aJ_2 + \lambda k\sqrt{J_2} + k^2bI_1 - k^2g(\bar{D}) = 0 \quad -$$

loading surface (15)

where \bar{D} is the damage parameter, $g(\bar{D})$ is the function of accumulated damage, J_2 is the invariant of deviatoric part of stress tensor, I_1 is the first invariant of the stress tensor, parameters a , b and λ are constants [7], while k is the shape coefficient. Accumulated damage is described by a tensile (D_t) and a compressive (D_c) damage parameters with two different damage loading surfaces up to the total failure. This model is useful for describing the behaviour of the structure under cycling loading paths.

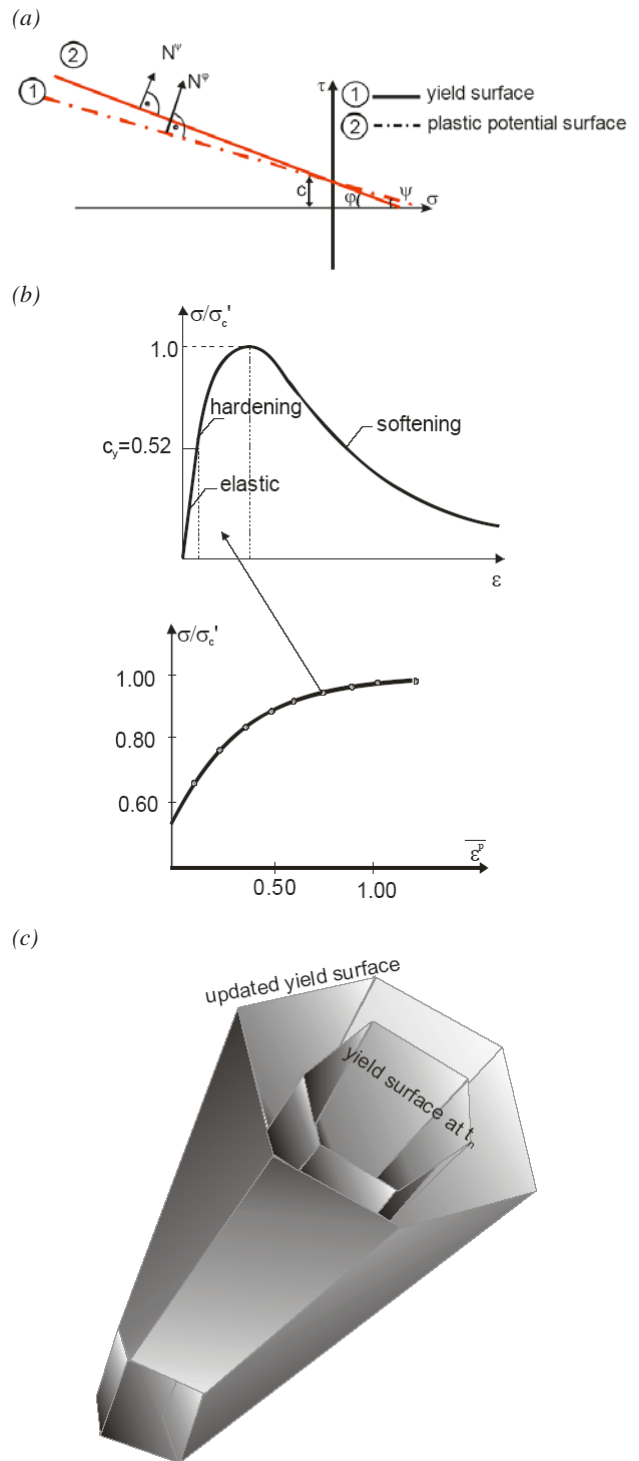


Fig. 6 Material model formulation for 3D analysis for concrete: (a) Graphical presentation of associated and non-associated flow rules; (b) Hardening and softening functions with respect to the total plastic strains; (c) Three-axial presentation of the yielded surface

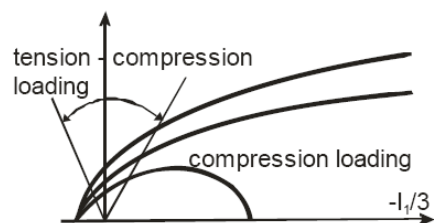


Fig. 7 Voyiadjis - Abu-Lebdech model [7]

Burlion model (Figure 8) [2] uses the yield function according to Needleman and Tvergaard [13] which is a modification of the yield function proposed by Gurson [14]. Yield criterion is described as:

$$f_{NT}(\sigma, \sigma_M, f^*) = \frac{3I_2}{\sigma_M^2} + 2g_1 f^* \cosh\left(g_2 \frac{I_1}{2\sigma_M}\right) - \left(1 + (g_3 f^*)^2\right) \quad (16)$$

where: I_1 and I_2 are the first and the second invariant of the stress tensor, σ_M is the equivalent yield stress, f^* is the volume fraction of voids, and g_1, g_2 and g_3 are model parameters. In the model, the variation of the void volume fraction f^* is controlled by the plastic flow. While f^* increases with void development in tension, it decreases with void closure in compression. In this model damage growth is associated to the evolution of porosity and to the evolution of micro-cracking at the same time (plasticity-damage coupling). From the algorithmic point of view, an explicit Forward Euler integration scheme is used for solving the evolution equations; thus only small step sizes should be applied.

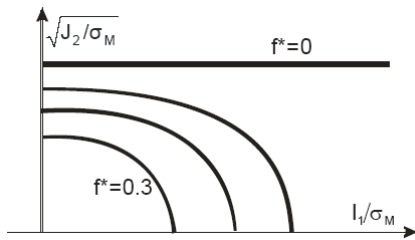


Fig. 8 Burlion model [2]

Kang model [15] uses three functions which define: hardening, softening and crack development for defining behaviour of concrete. This can be mathematically written as:

$$F(\xi, \rho, \theta) = F(\xi, \rho, \theta)_{crack} + F(\xi, \rho, k(qh))_{hard} + F(\xi, \rho, c(qs))_{soft} \quad (17)$$

Figure 9 shows development of the loading surfaces in deviatoric plane on few levels along hydrostatic axis.

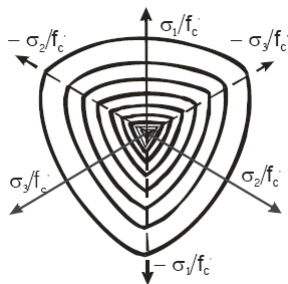


Fig. 9 Kang model

Shown model is useful for the description and the analysis of high reinforced concrete columns under combined longitudinal and transversal loading.

2.3 Parametric models

Ottosen four-parameter model [16] defines failure criterion by using all three stress invariants (I_1, J_2 and θ) and four parameters (a, b, k_1 and k_2) what is mathematically described as:

$$f(I_1, J_2, \theta) = aJ_2 + \lambda\sqrt{J_2} + bI_1 - 1 = 0 \quad (18)$$

where λ is the function of $\cos 3\theta$ defined as:

$$\lambda = \begin{cases} k_1 \cos\left[\frac{1}{3}\cos^{-1}(k_2 \cos 3\theta)\right] & \text{for } \cos 3\theta \geq 0 \\ k_1 \cos\left[\frac{\pi}{3}\cos^{-1}(-k_2 \cos 3\theta)\right] & \text{for } \cos 3\theta \leq 0 \end{cases} \quad (19)$$

Parameters a, b, k_1 and k_2 are constants obtained from standard uniaxial tests for determining tensile $f_t'(\theta=0^\circ)$ and compressive $f_c'(\theta=60^\circ)$ strength, and interrelationship for the element under biaxial and triaxial stress state.

The failure surfaces in the deviatoric planes, described with Eq. (18), are quadratic parabolas which are convex if $a > 0$ and $b > 0$. These failure surfaces in the deviatoric planes fulfil conditions of symmetry and convexity and change the shapes from nearly triangular to nearly circular depending on the increase of the hydrostatic pressure. The model encompasses several known models as special cases for some predefined values of the a, b and λ . For the case $a=b=0$ and $\lambda=\text{konst}$ one can get von-Mises model, and for $a=0$ and $\lambda=\text{konst}$ one can get Drucker-Prager model, both with circular failure surfaces.

This four-parameter model is valid for a wide range of stress combinations. In its mathematical form it is suitable for the implementation into computer programmes but demand large number of material parameters which can be obtained from experimental investigations only [1].

Hsieh-Ting-Chen four-parameter model (Figure 10) [17] improve Ottosen four-parameter model by introducing simpler equation for λ :

$$\lambda(\theta) = b \cos \theta + c \quad \text{for } |\theta| \leq 60^\circ \quad (20)$$

where b and c are constants.

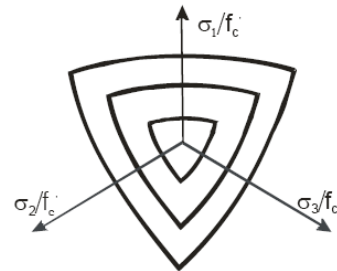


Fig. 10 Hsieh-Ting-Chen four parameter model

Replacing λ in Eq. (19), i.e. failure criterion in Ottosen four-parameter model, and using Haigh-Westergard coordinates yields a failure function of the form [1]:

$$f(\xi, \rho, \theta) = a\rho^2 + (b \cos \theta + c)\rho + d\xi - 1 = 0 \quad (21)$$

where a, b, c and d are material constants. Noting that $\rho \cos \theta = (\sqrt{3/2}\sigma_1 - I_1/\sqrt{6})$ in the Haigh-Westergard space, we can rewrite Eq. (21) in the terms of the stress invariants I_1, J_2 and J_3 with the four new material constants A, B, C and D as:

$$AJ_2 + B\sqrt{J_2} + C\sigma_1 + DI_1 - 1 = 0 \quad (22)$$

It is interesting to note that functional form of Eq. (22) appears to be a linear combination of three well-known failure criteria, namely, the von Mises, the Drucker-Prager and the Rankine criteria. The material parameters A, B, C and D are determined by the use of biaxial tests of Kupfer et al. [18] and of the triaxial tests of Mills and Zimmerman [19]. They are determined from four failure states: (i) uniaxial compressive strength f_c' ; (ii) uniaxial tensile strength $f_t' = 0.1 f_c'$; (iii) equally biaxial compressive strength $f_{bc}' = 1.15 f_c'$; and (iv) stress state $(\sigma_{oct}/f_c', \tau_{oct}/f_c') = (-1.95, 1.6)$ on the compressive meridian ($\theta = 60^\circ$). Finally, the values of these four constants are: $A = 2.0108, B = 0.9714, C = 9.1412$ and $D = 0.2312$.

Willam-Warnke five-parameter model [20] has curved tensile and compressive meridians expressed by quadratic parabolas of the form:

$$\begin{aligned} \sigma_m &= a_0 + a_1\rho_t + a_2\rho_t^2, \\ \sigma_m &= b_0 + b_1\rho_c + b_2\rho_c^2 \end{aligned} \quad (23)$$

where: σ_m is the mean normal stress obtained from $\sigma_m = I_1/3$, ρ_t and ρ_c are the stress components perpendicular on the hydrostatic axis at planes $\theta = 0^\circ$ for tensile stresses and $\theta = 60^\circ$ for compressive stresses, respectively, and $a_0, a_1, a_2, b_0, b_1,$ and b_2 are material constants obtained by using five typical tests for this kind of analysis.

Stresses σ_m, ρ_t and ρ_c are normalized with uniaxial compressive strength f_c' and are shown in Figure 11 in the coordinate system $\sigma_m/f_c', \rho_t/f_c', \rho_c/f_c'$.

Willam-Warnke failure curves are convex and smooth everywhere (Figures 11 and 12) [1]. Due to the threefold symmetry, it is only necessary to consider the interval $0 \leq \theta \leq 60^\circ$. The symmetry conditions at angle $\theta = 0^\circ$ and $\theta = 60^\circ$ (Figure 12) require that the position vectors ρ_t and ρ_c must be perpendicular to the ellipse at the points $P_1(0, b)$ and $P_2(m, n)$, respectively. To satisfy always the normality condition at point P_1 the y -axis have to coincide with the position vector ρ_t . The outward normal unit vector to the ellipse at point $P_2(m, n)$ must form an angle of 30° with the x -axis. Using aforementioned conditions, the half-axes a and b in terms of the position vectors ρ_t and ρ_c can be determined, and after some algebra, the radius $\rho(\theta)$ can be expressed in terms of parameters ρ_t and ρ_c as:

$$\rho(\theta) = \frac{2\rho_c(\rho_c^2 - \rho_t^2)\cos\theta + \rho_c(2\rho_t - \rho_c)\left[4(\rho_c^2 - \rho_t^2)\cos^2\theta + 5\rho_t^2 - 4\rho_t\rho_c\right]^{1/2}}{4(\rho_c^2 - \rho_t^2)\cos^2\theta + (\rho_c - 2\rho_t)^2} \quad (24)$$

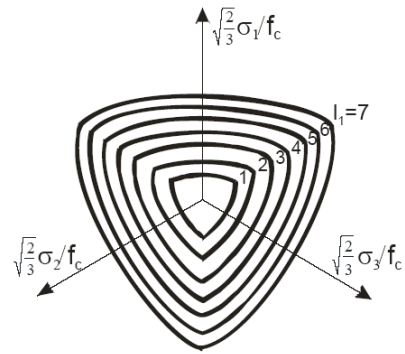


Fig. 11 Willam-Warnke five-parameter model

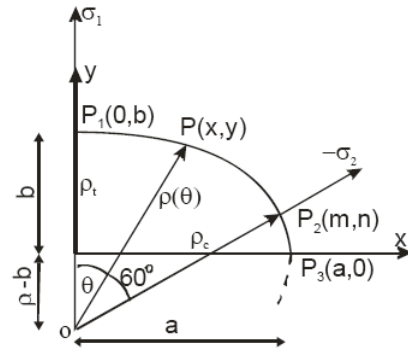


Fig. 12 Trace of the deviatoric section of the Willam-Warnke five-parameter failure surface for the interval $0 \leq \theta \leq 60^\circ$

Two limiting cases of Eq. (24) can be observed. First, for relation $\rho_t/\rho_c = 1$ (or, equivalently, $a = b$), the ellipse degenerates into a circle (similar to the deviatoric trace of the von Mises or Drucker-Prager models). Second, when ratio ρ_t/ρ_c approaches the value $1/2$ (or, equivalently, $a/b \rightarrow \infty$), the deviatoric trace becomes nearly triangular (similar to that for the maximum tensile stress criterion). Therefore, both convexity and smoothness of the failure curve (Figure 9) can be assured in the interval $1/2 \leq \rho_t/\rho_c \leq 1$. The five parameters of the failure function of the Willam-Warnke five-parameter model are now determined by the following five failure tests:

- * uniaxial compression strength f_c'
- * uniaxial tensile strength $f_t' = 0.1 f_c'$
- * biaxial compressive strength $f_{bc}' = 1.15 f_c'$
- * confined biaxial compression strength with $(\sigma_1 > \sigma_2 = \sigma_3)$ where $(\sigma_m, \rho_t) = (-1.95 f_c', 2.77 f_c')$
- * confined biaxial compression strength with $(\sigma_1 = \sigma_2 > \sigma_3)$ where $(\sigma_m, \rho_c) = (-3.9 f_c', 3.461 f_c')$

2.4 Micro-plane models

In the micro-plane approach, proposed by Bažant et al. [21] what is an improvement of the previously developed classical micro-plane model, the constitutive model of concrete is defined by relations between stresses and strains acting on a plane of arbitrary orientation the so-called micro-plane (Figure 13). Every plane is defined with its unit normal vector \mathbf{n} , i.e. with i -th unit normal vector for that micro-plane, $\mathbf{n}_i = [n_x^i \ n_y^i \ n_z^i]^T$. The model use kinematic constraint, which defines the strain vector \mathbf{e}_i on the i -th micro-plane with unit normal \mathbf{n}^i as $\mathbf{e}^i = \mathbf{n}^i \boldsymbol{\epsilon}$. Finally, the micro-plane stress vector is connected to the macroscopic stress tensor by using the principle of virtual work by the equation:

$$\sigma_{ij} = \frac{3}{2\pi} \int_{\Omega} (\sigma_N N_{ij} + \sigma_M M_{ij} + \sigma_L L_{ij}) d\Omega(N) \quad (25)$$

where σ_N is the normal stress on the micro-plane, σ_M and σ_L are the shear components in a plane normal to \mathbf{n} , and N_{ij} , M_{ij} and L_{ij} are symmetric tensors related to the direction of the micro-plane. Tensorial stress-strain laws are then obtained by averaging over all possible orientations of the micro-plane.

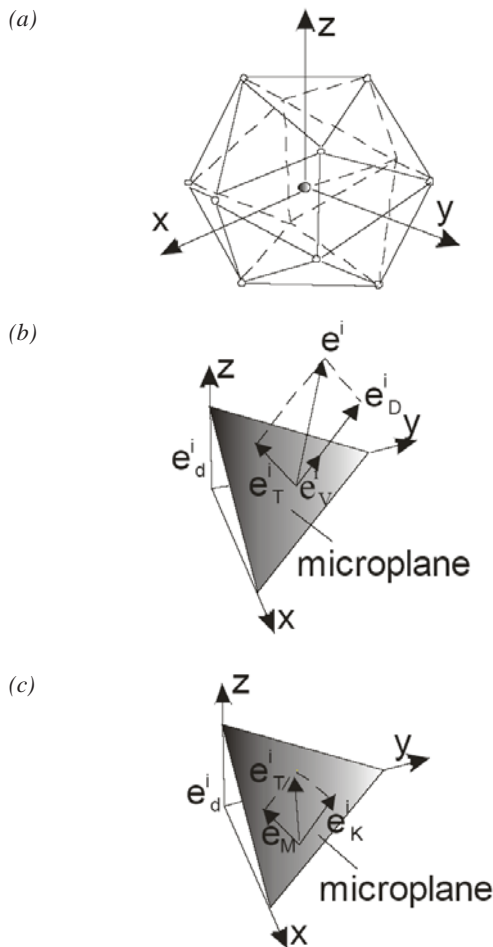


Figure 13. Micro-plane model: (a) discretization with 21 micro planes; (b) normal and shear strain component on the i -th micro-plane; (c) shear strain components on the i -th micro-plane [21]

The micro-plane models are certainly the most detailed and the best to describe the behaviour of concrete and concrete structures, because these models analyze this extremely heterogeneous material at the micro-level linking its behaviour at the macro-level [22]. However; due to the complexity of the description, a large number of planes in which the behaviour is analyzed and the high number of required parameters; they are not suitable for implementation in models which discretize the structure by composite finite elements; namely, they are not suitable for description of reinforced concrete and prestressed concrete cross-sections.

3. COMMENTS AND CONCLUSIONS

The need for a more realistic description of concrete behaviour has led to the development of a large number of models that provide a wide range of responses of this heterogeneous material to various loads and stresses.

This brief overview of some characteristic numerical models of concrete shows how difficult it is to form a model that will describe a non-linear behaviour, include a greater number of impacts arising from this behaviour, precisely define them mathematically, and in doing so use the material parameters that do not require further experimental investigations.

One can note that all presented models comprise a large number of parameters (material and model parameters) that require expensive experimental investigations, Table 2.

Table 2. Total number of required parameters for different concrete models

Constitutive model	Number of material parameters	Number of model parameters	Total number of required parameters
ELM	5	11	16
DP-RK	5	4	9
DP-TC	5	4	9
Ottosen	5	4	9
Willam-Warnke	5	5	10
Micro-plane	9	13	22

It is shown that modelling depends on what changes and what kind of behaviour is to be observed and analyzed and at what level (macro or micro). Regardless of how much the model is accurate and precise, it might not be a good choice for a problem that is to be described. If not appropriate model is selected, different problems may arise: mathematical (convergence of the procedure), physical (model does not include the dominant influence that shall be analyzed), or technical one when we are (still) limited

by the computer capacity that does not allow micro analysis in combination with different materials and composite finite elements. A brief overview of possibilities and limitations of described models, recommendations what model to apply in the analysis of particular problem and difficulties that might be encountered is given in Table 3.

ACKNOWLEDGEMENT

The partial financial support, provided by the Ministry of Science, Education and Sports of the Republic of Croatia under the projects Numerical and Experimental Modelling of Engineering Systems, Grant No. 0083061, and Numerical and Experimental Investigations of Engineering Structures Behaviour, Grant No. 083-0831541-1547, is gratefully acknowledged.

LITERATURE

[1] W.F. Chen and D.J. Han, *Plasticity for Structural Engineers*, Springer-Verlag, New York, 1988.
 [2] P. Pivonka, Constitutive modelling of triaxially loaded concrete considering large compressive stresses: application to pull-out test of anchor bolts, Ph.D. Thesis, Vienna University of Technology, Vienna, 2001.
 [3] M. Galić, Development of nonlinear numerical 3D model of reinforced and prestressed concrete structures, Ph.D. Thesis, University of Split, Faculty of Civil Engineering and Architecture, Split, 2006. (in Croatian)
 [4] G. D’Addeta, F. Kun, E. Ramm and H. Hermann, From solids to granulates-discrete element simulations of fracture and fragmentation processes in geomaterials, In: *Continuous and discontinuous modelling of cohesive – frictional materials*, Lecture Notes in Physics, Vol. 568, Springer, Berlin, pp. 231-258, 2001.

Table 3 An overview of described models – possibilities and limitations

<i>The model is to describe</i>	<i>Models based on the theory of elasticity</i>	<i>Models based on the theory of elasto-plasticity</i>	<i>Damage models</i>	<i>Models based on the theory of fracture mechanics</i>
<i>Strain history</i>	<i>Possible if hypoelastic model is used</i>	<i>Flow surfaces, hardening/softening function and the flow vector shall be defined</i>	<i>Can be used in combination with some plastic models</i>	<i>Possible if certain material parameters are included</i>
<i>Anisotropic behaviour; hydrostatic and deviator responses to be included</i>	<i>Possible if hypoelastic model is used</i>	<i>Anisotropic load surface shall be defined</i>	<i>Applicable for distributed / smeared cracks</i>	<i>It has not been tested</i>
<i>Post-yield stress behaviour</i>	<i>Possible if secant stiffness modulus is used</i>	<i>Possible if strain is defined by functions on the load surface and hardening / softening curve</i>	<i>Not developed enough</i>	<i>Well describes changes under dominant tensile stresses</i>
<i>Damages (changes of elastic constants in the stiffness matrix)</i>	<i>The model can be used without significant limitations</i>	<i>It is not possible to use the model based on the classical theory of plasticity</i>	<i>A good description for distributed / smeared cracks</i>	<i>Not formulated for tension-compression domain</i>
<i>Behaviour under cyclic load</i>	<i>The model can be used without limitations</i>	<i>Possible if it involves elastic behaviour at unloading</i>	<i>It has not been used so far for description of this behaviour</i>	<i>Possible if it involves elastic behaviour at unloading</i>
<i>Development of cracks</i>	<i>Possible if hypoelastic model is used</i>	<i>Possible if cracks are described according to the assumptions of anisotropic or orthotropic plasticity</i>	<i>Possible if the cracks are well distributed</i>	<i>Mainly used to describe discrete cracks</i>

- [5] G. Etse, Theoretische und numerische Untersuchung zum diffusen und lokalisierten Versagen in Beton, Ph.D. Thesis, University of Karlsruhe, Karlsruhe, 1992. (in German)
- [6] G. Etse and K. Willam, Fracture energy formulation for inelastic behaviour of plain concrete, *ASCE Journal of Engineering Mechanics*, Vol. 120, No. 9, pp. 1983-2011, 1994.
- [7] G.Z. Voyiadjis and T.M. Abu-Lebdeh, Damage model for concrete using bounding surface concept, *ACSE Journal of Engineering Mechanics*, Vol. 119, No. 9, pp. 1865-1885, 1993.
- [8] H. Menrath, A. Haufe and E. Ramm, A model for composite steel-concrete structures, Proc. EURO-C 1998 Conf. on Computational Modelling of Concrete Structures, Badgastein, March/April 1998, Eds.: R. de Borst, N. Biazania; H.A. Mang and G. Meschke, Balkema A.A., Rotterdam, Vol. 1, pp. 33-42, 1998.
- [9] G. Meschke, R. Lackner and H.A. Mang, An isotropic elastoplastic-damage model for plain concrete, *International Journal for Numerical Methods in Engineering*, Vol. 42, No. 4, pp. 703-727, 1998.
- [10] M. Galić, P. Marović and Ž. Nikolić, Modified Mohr-Coulomb – Rankine material model for concrete, *Engineering Computations*, Vol. 28, No. 7, pp. 853-887, 2011.
- [11] G. Meschke, Synthese aus konstitutivem Modellieren von Beton mittels dreiaxialer, elastoplastischer Werkstoffmodelle und Finite-Elemente-Analysen dickwandiger Stahlbetonkonstruktionen, Ph.D. Thesis, Vienna University of Technology, Vienna, 1989. (in German)
- [12] A. van Gysel and L. Taerwe, Analytical formulation of the complete stress-strain curve for high strength concrete, *Materials and Structures*, Vol. 29, No. 193, pp. 529-533, 1996.
- [13] A. Needleman and V. Tvergaard, An analysis of ductile rupture in notched bars, *Mechanics and Physics of Solids*, Vol. 32, No. 6, pp. 461-490, 1984.
- [14] N. El-Mezaini and E. Citipitioglu, Finite element analysis of prestressed and reinforced concrete structures, *ASCE Journal of Structural Engineering*, Vol. 117, No. 10, pp. 2851-2864, 1991.
- [15] H.D. Kang, K. Willam, B. Shing and E. Spacone, Failure analysis of R/C columns using a triaxial concrete model, *Computers & Structures*, Vol. 77, No. 5, pp. 423-440, 2000.
- [16] N.S. Ottosen, A failure criterion for concrete, *ASCE Journal of Engineering Mechanics Division*, Vol. 103, No. 4, pp. 527-533, 1977.
- [17] S.S. Hsieh, E.C. Ting and W.F. Chen, A plasticity-fracture model for concrete, *Int. J. of Solids and Structures*, Vol. 18, No. 3, pp. 181-197, 1982.
- [18] H. Kupfer, H.K. Hilsdorf and H. Rusch, Behaviour of concrete under biaxial stresses, *ACI Journal*, Vol. 66, No. 8, pp. 656-666, 1969.
- [19] L.L. Mills and R.M. Zimmerman, Compressive strength of plain concrete under multiaxial loading conditions, *ACI Journal*, Vol. 67, No. 10, pp. 802-807, 1970.
- [20] K.J. Willam and E.P. Warnke, Constitutive model for the triaxial behaviour of concrete, IABSE Report, Vol. 19, Proc. IABSE Colloquium on Concrete Structures Subjected to Triaxial Stresses, ISMES, Bergamo, pp. 1-30, 1974.
- [21] Z. Bažant, Y. Xiang and P.C. Prat, Microplane model for concrete, Part I: Stress-strain boundaries and finite strain, *ASCE Journal of Engineering Mechanics*, Vol. 122, No. 3, pp. 245-254, 1996.
- [22] J. Ožbolt, L. Yijun and I. Kožar, Microplane model for concrete with related kinematic constraint, *Int. J. Solids and Structures*, Vol. 38, No. 16, pp. 2683-2711, 2001.

PREGLED NEKIH KARAKTERISTIČNIH NUMERIČKIH MODELA BETONA

SAŽETAK

Na osnovu eksperimentalnih ispitivanja ponašanja betonskih, armiranobetonskih i prednapetih konstrukcija zapažene su razne pojave, u prvom redu, izrazito nelinearno i neelastično ponašanje betona. Kako je teško obuhvatiti sve pojave i promjene koje se javljaju u betonu, razvio se veliki broj numeričkih modela betona za opisivanje različitih stanja problema, s težnjom da se u tim analizama uključe promjene koje su dominantne u promatranom problemu. U ovom radu dat će se kratki pregled nekih karakterističnih do sada razvijenih numeričkih modela betona s kratkim osvrtom na njihove prednosti i nedostatke. Izvršena je podjela tih modela ovisno o načinu formuliranja zakona ponašanja. Modeli su odabrani tako da pokažu raznolikost načina modeliranja te specifičnosti njihove primjene.

Ključne riječi: beton, konstitutivni model betona, numerički model betona, plastičnost.